A mathematical model of the global ionospheric electric field generated by thunderstorms

Article

Accepted Version

A MATHEMATICAL MODEL OF THE GLOBAL IONOSPHERIC ELECTRIC FIELD GENERATED BY THUNDERSTORMS

© **2022** V.V. Denisenko[1,*], M.J. Rycroft[2], R.G. Harrison[3]

[1] Institute of Computational Modelling RAS SB, Krasnoyarsk, Russia

[2] CAESAR Consultancy, Cambridge, UK
[3] Department of Meteorology, University of Reading, Reading, UK
**E-mail:* denisen@icm.krasn.ru

A model is created for the thunderstorm-related ionospheric part of the global electric circuit in January. This current system consists of four equatorial electrojets, day- and night-time, westward and eastward, up to 120 A. Data on the atmospheric fair weather electric field obtained during Carnegie cruise VII are plotted as a two dimensional map in UT and month coordinates to show both UT and seasonal variations.

INTRODUCTION

There are several mechanisms by which an ionospheric electric field may be generated. The currents produced by all these generators are referred to as the global electric circuit (GEC) [1]. Here we study only that part of the GEC which is generated by the currents flowing up from the atmosphere. Although numerous articles analyze the thunderstorm-related part of the GEC, its ionospheric part is still insufficiently studied.

The objective of this paper is to present our model for electric fields and currents which constitute the ionospheric part of the thunderstorm-related part of the GEC. The first results of our modelling efforts were presented in [2], with corrections of misprints [3]. An important feature of the global ionospheric currents is their concentration near the geomagnetic equator, as shown in [4]. Here we briefly describe the model, and then we present some new results which are obtained using a model for the global distribution of thunderstorms [5] obtained from the ground-based World Wide Lightning Location Network (WWLLN) [6].

MODEL OF THE GLOBAL IONOSPHERIC CONDUCTOR

Our model of a global conductor consisting of the atmosphere, ionosphere, magnetosphere and lithosphere, constructed to describe the GEC with acceptable simplifications, is described in detail in the article [2]. We consider the atmosphere, ionosphere and magnetosphere as a single conductor, bounded from below by an ideal conductor, including oceans and land. The basic equations for a stationary electric field $\boldsymbol{E}$ and current density $\boldsymbol{j}$ are Faraday's law, the charge conservation law and Ohm's law with the conductivity tensor $\hat{\boldsymbol{\sigma}}$. The electric potential V is introduced, for which the system of equations is reduced to the current continuity equation

$$-div(\hat{\boldsymbol{\sigma}}\, grad\, V) = Q. \qquad (1)$$

We use spherical geomagnetic coordinates θ_m, φ_m, geomagnetic latitude $\lambda_m = \frac{\pi}{2} - \theta_m$ and altitude above mean sea level h. The conductivity of the Earth's ionosphere is a gyrotropic tensor, one axis of which is determined by the direction of magnetic induction $\boldsymbol{B}$. We use components of vectors parallel and normal to $\boldsymbol{B}$, which we mark with the symbols $\parallel$ and $\perp$, while $B = |\boldsymbol{B}|$. Then Ohm 's law has the form

Denisenko V.V, Rycroft M.J., Harrison R.G. Mathematical model of the global ionospheric electric field generated by thunderstorms *Bulletin of the Russian Academy of Sciences: Physics*. 2023. V. 87(1). 118-123.
DOI:10.3103/S1062873822700277

$$\boldsymbol{j}_{\parallel} = \sigma_{\parallel}\boldsymbol{E}_{\parallel}, \quad \boldsymbol{j}_{\perp} = \sigma_P\boldsymbol{E}_{\perp} - \sigma_H[\boldsymbol{E}_{\perp} \times \boldsymbol{B}]/B \tag{2}$$

with Hall (σ_H), Pedersen (σ_P) and field-aligned ($\sigma_{\parallel}$) conductivities. The conductivities are calculated using empirical models IRI-2016, MSIS 1990 E and IGRF. Since the field-aligned conductivity $\sigma_{\parallel}$ in the ionosphere is several orders of magnitude greater than σ_P, σ_H, it is possible to reduce the three-dimensional model to a two-dimensional one [7]. Integrating Ohm's law (2) along the magnetic field line, we obtain the total current density through the magnetic field line $\boldsymbol{J}_{\perp}$. If the magnetic field lines were parallel straight lines, then $\boldsymbol{E}_{\perp}$ would be constant during this integration, and

$$\boldsymbol{J}_{\perp} = \begin{pmatrix} \Sigma_P & \Sigma_H \\ -\Sigma_H & \Sigma_P \end{pmatrix} \boldsymbol{E}_{\perp}, \tag{3}$$

with Pedersen and Hall conductances Σ_P, Σ_H, which are obtained from the local Pedersen and Hall conductivities σ_P, σ_H by integration along the magnetic field line. Magnetic field lines are not parallel straight lines, and this introduces some geometric factors into the integration. We also use the Cowling conductance $\Sigma_C = \Sigma_P + \Sigma_H^2/\Sigma_P$, which is most important at low latitudes.

The charge conservation law (1) in the two-dimensional model is satisfied in the form integrated along the magnetic field line. For the numerical solution of the problem, it is useful to construct some reference region on a plane with Cartesian coordinates x, y, the points of which identify all the magnetic field lines under consideration. In the dipolar approximation of the geomagnetic field the two-dimensional electrical current continuity equation in such a domain can be written as

$$-\frac{\partial}{\partial x}\left(\Sigma_P \frac{\partial V}{\partial x} + \Sigma_H \frac{\partial V}{\partial y}\right) - \frac{\partial}{\partial y}\left(-\Sigma_H \frac{\partial V}{\partial x} + \Sigma_P \frac{\partial V}{\partial y}\right) = Q, \tag{4}$$

where Q is determined by atmospheric currents entering the ionosphere through the ends of the magnetic field line in the Northern and Southern hemispheres. For a real geomagnetic field, the coefficients in (4) have a more complicated form [7]. Consideration of the conductors in the magnetosphere [8] shows that the auroral zones are equivalent to almost ideal conductors, since they are connected in parallel both to each other and to good magnetospheric conductors. We consider them to be an ideal conductor with zero electric potential $V = 0$, which gives the Dirichlet boundary condition. The second boundary of the conductor is formed by the lowest magnetic field lines, considered as ionospheric. The current from the atmosphere is imposed. We obtain a mixed boundary value problem for a partial differential equation (4), which is an equation of elliptic type. It has a unique solution [9].

THE MODEL OF THE GLOBAL THUNDERSTORM GENERATOR

The generator in the GEC can be considered as the sum of all thunderstorms on the Earth [10]. Their cumulative parameter is the total conductive current into the ionosphere. Unfortunately, we have no instrument to measure this current. Thus, we must use the procedure [5] described briefly here.

At first, we take the electric field strength near the ocean surface under fair weather conditions for the studied moment of time by the Carnegie map described in the next section. This field E_0 and a 1-D model of atmospheric conductivity gives the potential difference between the surface and the ionosphere U_0. Then we obtain fair weather currents all over the globe and, by integration, get the total fair weather current from the ionosphere I_0. The parameter $R = U_0/I_0$ is the total resistance of the atmosphere.

Charge conservation for the stationary case means the same current from the thunderstorms to the ionosphere $I_{storm} = I_0$. Because the distribution of the thunderstorm current over the Earth is

Denisenko V.V, Rycroft M.J., Harrison R.G. Mathematical model of the global ionospheric electric field generated by thunderstorms *Bulletin of the Russian Academy of Sciences: Physics*. 2023. V. 87(1). 118-123.
DOI:10.3103/S1062873822700277

unknown, it is replaced by the global distribution of lightning activity. Indeed, we explicitly assume that the current into the ionosphere and the number of flashes of lightning are both linearly proportional to some hidden parameter that characterizes the thunderstorm activity. We use the model [5] of the global distribution of thunderstorm activity obtained from the global network of ground-based very low frequency radio receivers WWLLN.

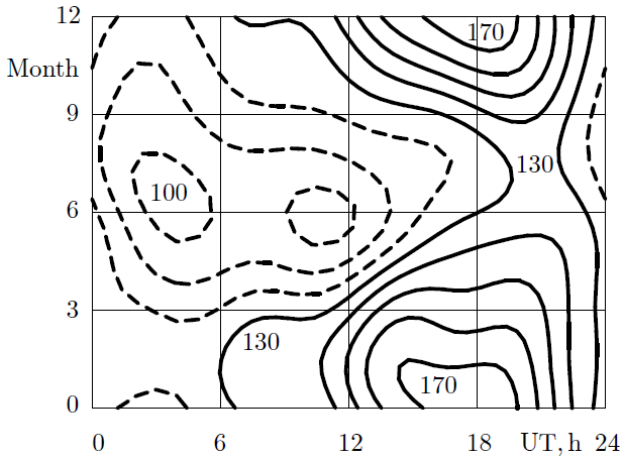

Fig. 1. The vertical electric field above the ocean surface derived from the Carnegie Cruise VII data [11]. Contours of E_0 depending on time (UT) and month are plotted at intervals of 10 V/m. Dashed lines correspond to $E_0 \leq 120$ V/m.

In the article [11], approximations of the Carnegie curves, i.e. E_0 as a function of UT, obtained for different seasons during Cruise VII are constructed. The approximating functions were chosen to be of the form

$$E_z(t) = -A_0 - \sum_{n=1}^{4} A_n \sin(nt \cdot 15^o + \varphi_n), \qquad (5)$$

where E_z is the electric field strength above the ocean surface, and t- is the universal time (UT) in hours. The values of the coefficients A_n and phases φ_n were given in Table 4 in [11] with averaging over three months, NDJ (November, December, January) and similarly, denoted FMA, MJJ, ASO.

It is convenient to analyze the seasonal dependence if we move from these four time functions $E_z(t)$ to a single function $E_z(m,t)$, where the parameter m describes the time during the year, e.g., in months. We consider the parameter m not discrete, but continuously changing in the interval $0 < m < 12$.

To determine $E_z(m,t)$, it is necessary to determine the dependence of parameters (5) on m, for example, $A_0(m)$. It is natural to assume that the values of parameters (1) given in [1] are obtained as averages for these seasons, for example:

$$A_0^{\mathrm{NDJ}} = \frac{1}{3}\int_{-2}^{1} A_0(m)\,dm,\ A_0^{\mathrm{FMA}} = \frac{1}{3}\int_{1}^{4} A_0(m)\,dm,$$
$$A_0^{\mathrm{MJJ}} = \frac{1}{3}\int_{4}^{7} A_0(m)\,dm,\ A_0^{\mathrm{ASO}} = \frac{1}{3}\int_{7}^{10} A_0(m)\,dm. \qquad (6)$$

The desired approximating function $A_0(m)$ must satisfy these equations. We can use a trigonometric polynomial

$$A_0(m) = a + b\cos(2\pi(m-0.5)/12) + c\sin(2\pi(m-0.5)/12) + e\cos(4\pi(m-0.5)/12). \qquad (7)$$

A half-month shift corresponds to a shift in the averages (6) and allows us not to include in (7) another term $\sin(4\pi(m-0.5)/12)$, since ~~its~~ average values over each of four intervals (6) are zero. It is easy to calculate the average values of the function (7) over each interval. Substituting them into

Denisenko V.V, Rycroft M.J., Harrison R.G. Mathematical model of the global ionospheric electric field generated by thunderstorms *Bulletin of the Russian Academy of Sciences: Physics*. 2023. V. 87(1). 118-123.
DOI:10.3103/S1062873822700277

equations (6) we obtain four linear algebraic equations for four unknowns a, b, c, e. The solution of these equations is

$$a = (A_0^{\mathrm{NDJ}} + A_0^{\mathrm{FMA}} + A_0^{\mathrm{MJJ}} + A_0^{\mathrm{ASO}})/4,\ b = (A_0^{\mathrm{NDJ}} - A_0^{\mathrm{MJJ}})\pi/(4\sqrt{2}),$$
$$c = (A_0^{\mathrm{FMA}} - A_0^{\mathrm{ASO}})\pi/(4\sqrt{2}),\ e = (A_0^{\mathrm{NDJ}} - A_0^{\mathrm{FMA}} + A_0^{\mathrm{MJJ}} - A_0^{\mathrm{ASO}})\pi/16. \quad (8)$$

Similarly, we calculate the coefficients of polynomials of the form (7) for the remaining eight functions. Substituting the obtained nine functions $A_0(m), \ldots, \varphi_4(m)$ into the representation (5), we obtain the desired function $E_z(m, t)$. Its contours are shown in Fig. 1. By construction, averaging over three months gives a Carnegie curve for this period. Fig. 1 can be called a Carnegie VII map. It gives a visual representation of not only UT variations, like the Carnegie curve, but also variations throughout the year.

As can be seen in Fig. 1, the electric field strength in the atmosphere above the ocean is minimal (about 100 V/m) in the period 02-12 UT in June-July and maximum (up to 170 V/m) in the period 15-19 UT in January. The latter circumstance determines the choice of January 1 for a detailed presentation of the simulation results in this article.

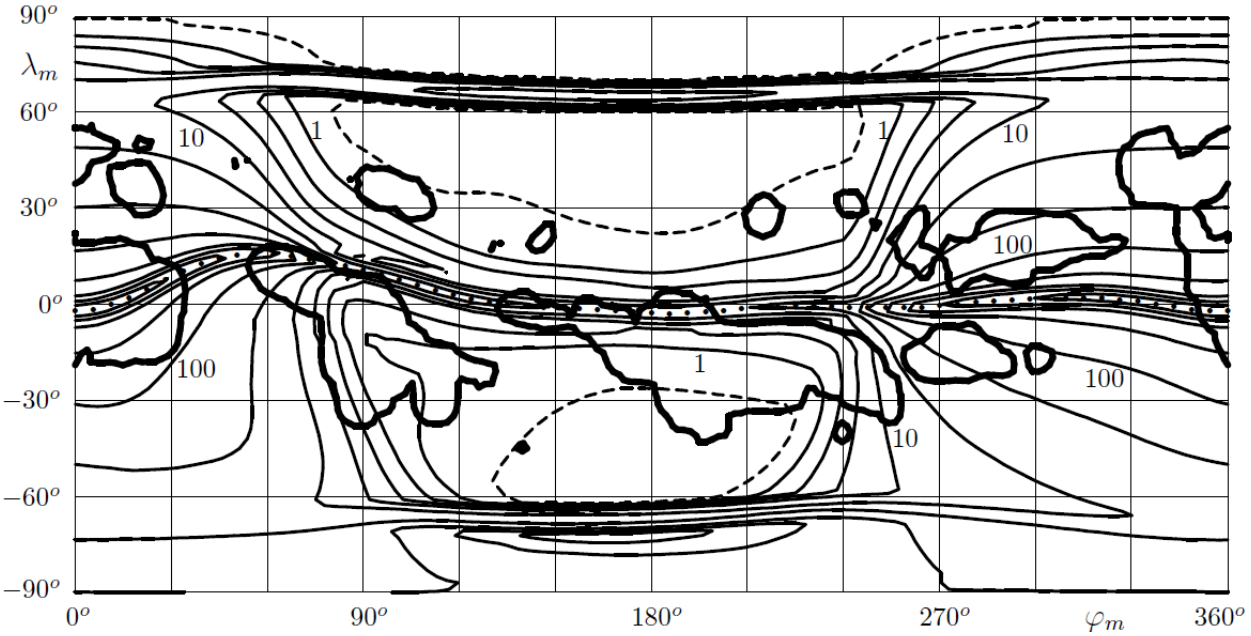

Fig. 2. The global distribution of the Cowling conductance Σ_C shown for 18:00 UT on January 1 under low solar activity conditions. The bold contours separate thunderstorm regions where $J_{atm} > 0$, and the geomagnetic equator is shown with dots.

As described above we obtain the global distribution of thunderstorm currents to the ionosphere obtained for the first day of a year when Fig. 1 shows the maximum value of $E_0 = 177$ V/m at 18 UT. Then we add fair weather currents which have the opposite direction, $J_{atm} < 0$. The bold contours in Fig. 2 separate thunderstorm regions where $J_{atm} > 0$.

Since the Carnegie map presents measurements above the ocean we use atmospheric parameters which are $\sigma(0)$=3.09·10^{-14} S/m and $\Sigma(\lambda, \varphi)$=1.09·10^{-17} S in accordance with the model [2]. For $E_0 = 177$ V/m we obtain $U_0 = 502$ kV and I_{storm}=2.79 kA when R=180 Ohm. If we use parameters corresponding to the ground $\sigma(0)$=1.54·10^{-14} S/m and $\Sigma(\lambda, \varphi)$=0.80·10^{-17} S for the same E_0 we would obtain $U_0 = 340$ kV and I_{storm}=1.89 kA.

The solution for the mixed boundary value problem of equation (8) in the main part of the ionosphere at 18 UTC is presented in Fig. 3. The distribution of the electric potential $V(\varphi_m, \lambda_m)$ at the

Denisenko V.V, Rycroft M.J., Harrison R.G. Mathematical model of the global ionospheric electric field generated by thunderstorms *Bulletin of the Russian Academy of Sciences: Physics*. 2023. V. 87(1). 118-123.
DOI:10.3103/S1062873822700277

height h =120 km in the ionosphere is shown by the positions of the equipotentials, which are plotted with a contour interval of 20 V. For low values of $V < 40$ V, the contour interval is set to 4 V; in Fig. 3, these are shown as thin lines, and dashed lines mean negative values.

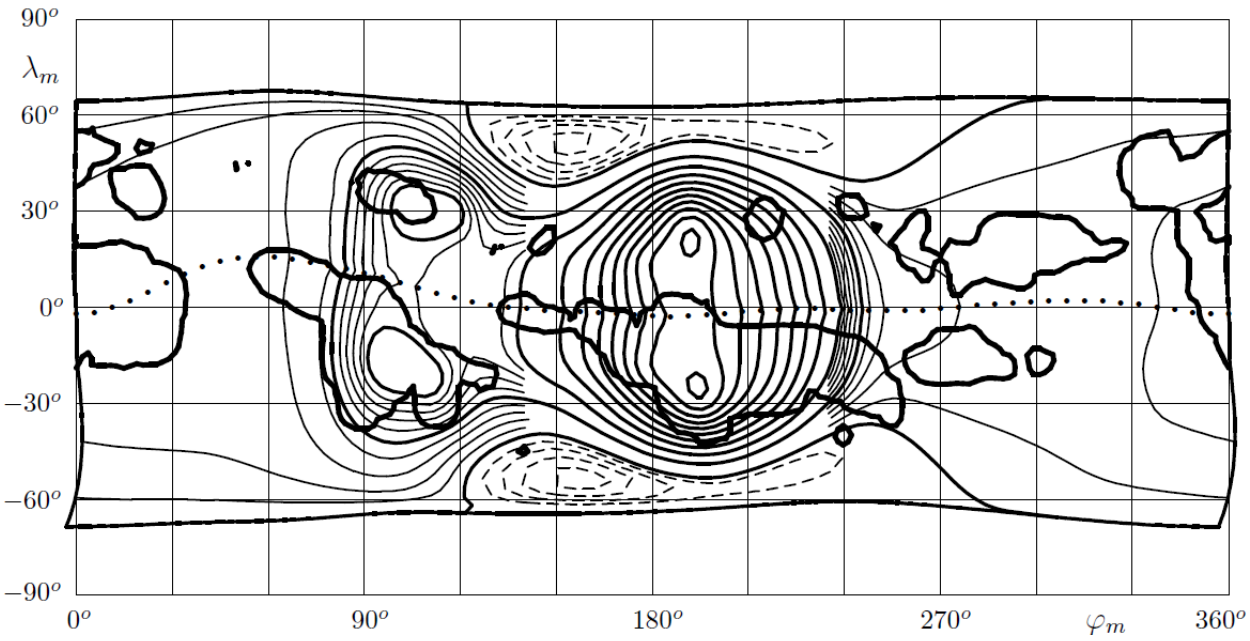

Fig. 3. Distribution of the electric potential at 120 km height in the ionosphere. Equipotentials are plotted with a contour interval of 20 V. For low values of $V < 40$ V, the contour interval is set to 4 V, and shown as thin lines. Dashed lines correspond to negative values of potential. The bold contours separate thunderstorm regions where $J_{atm} > 0$. The map is calculated for January 1 under low solar activity conditions at the considered point in time, 18:00 UT. The geomagnetic equator is shown with dots.

The maximum potential difference at 120 km altitude is about 220 V. It is three orders of magnitude smaller than the voltage between the ground and the ionosphere that is 502 kV in the model. The corresponding electric field strength is also small. Its horizontal component does not exceed 90 μV/m. Nevertheless, it is this small electric field which provides the distribution of the ionospheric currents which closes the currents from and to the atmosphere.

The position of the maximum value of the ionospheric potential $V = 205$ V corresponds to the large thunderstorm generator over North-Western Australia. We see only a slight enhancement of the potential above other thunderstorm regions because of the large day-time ionospheric conductivity (near the equator, local midday, at φ_m =340°). Fig. 3 demonstrates a natural property of the electric field strength: it is much larger in the night-time ionosphere due to the small ionospheric conductivity.

Let us now pay attention to the vicinity of the geomagnetic equator where the magnetic field $\boldsymbol{B}$ has a zero vertical component by definition. The geomagnetic equator is shown with dots in Fig. 2, 3. The equipotentials are normal to the geomagnetic equator. Strictly speaking, they are parallel to the magnetic field $\boldsymbol{B}$, and the direction of $\boldsymbol{B}$ is exactly normal to the geomagnetic equator only for a dipolar field. We see variations of the potential along the geomagnetic equator in Fig. 3 which imply a non zero $E_{\boldsymbol{\varphi}}$ component of the electric field strength.

Due to the substantial increase of the conductance at the geomagnetic equator, $E_{\boldsymbol{\varphi}}$ produces the equatorial electrojets [12]. Strictly speaking we need the component $E_{\boldsymbol{jet}}$ that is normal to the magnetic

field and does not differ much from E_{φ}. This field varies slightly with height at the magnetic field lines whose tops are below 200 km; it does not exceed 40 μV/m as seen in Fig. 4.

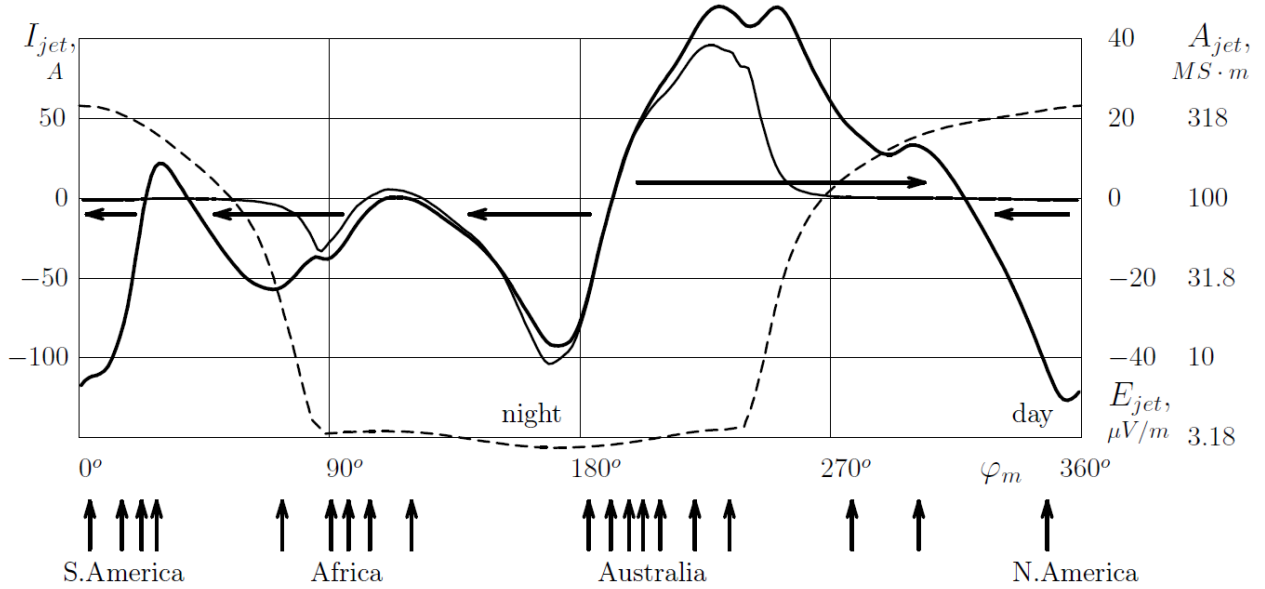

Fig. 4. The current of the electrojets $I_{jet}(\varphi_m)$ (bold line), the electric field component $E_{jet}(\varphi_m)$ (thin line), and the conductance of the electrojet area $A_{jet}(\varphi_m)$ shown on a logarithmic scale (dashed line). Horizontal arrows show the directions of the electrojets in the ionosphere. Vertical arrows mark the currents to the ionosphere from the thunderstorm regions; each arrow corresponds to 100 A near that meridian.

The electrojet current I_{jet} can be obtained by numerical integration over the height interval $90 < H < 135$ km [12]. Integration of the Cowling conductance over the same range of heights gives the total conductance of the electrojet area A_{jet}. The electrojet current is shown by the bold line in Fig. 4. The directions of the electrojets are also shown with horizontal arrows (positive current being eastward). Vertical arrows mark currents up to the ionosphere from the major thunderstorm regions, each arrow corresponding to 100 A at the sector. A large portion is produced in the huge thunderstorm region that contains North-West Australia and South-East Asia. This region defines the main eastward electrojet to the East from the region (up to 120 A) and the strong westward electrojet to the West from it (up to 90 A). These directions mean that the charges delivered to the ionosphere from the atmosphere diverge by the ionospheric currents, including these equatorial electrojets.

CONCLUSIONS

A model of the thunderstorm-related ionospheric part of the GEC at 18 UTC in January has been created. This current system contains four equatorial electrojets, day- and night-time, westward and eastward, with currents as large as 120 A. They produce magnetic perturbations on the ground, which are estimated to be in the 0.1 nT range. In principle, these magnetic perturbations could be measured at the night-time geomagnetic equator where they may not be hidden by strong electrojets which are produced by neutral wind driven ionospheric and/or magnetospheric generators. The data from a Carnegie cruise are presented in the form of a plot in UT and month coordinates to show both UT and seasonal variations; Fig. 1 is plotted for Carnegie cruise VII.

Denisenko V.V, Rycroft M.J., Harrison R.G. Mathematical model of the global ionospheric electric field generated by thunderstorms *Bulletin of the Russian Academy of Sciences: Physics*. 2023. V. 87(1). 118-123.
DOI:10.3103/S1062873822700277

This investigation was performed with the financial support of the Russian Science Foundation Grant No. 21-17-00208.

BIBLIOGRAPHY

1. *Hays P.B., Roble R.G.* // J. Geophys. Res. 1979. V. 84. No. A7. P. 3291.
2. *Denisenko V.V., Rycroft M.J., Harrison R.G.* // Surv. Geophys. 2019. V. 40. No. 1. P. 1.
3. *Denisenko V.V., Rycroft M.J., Harrison R.G.* // Surv. Geophys. 2019. V. 40. No. 1. P. 37.
4. *Denisenko V.V., Rycroft M.J.* // J. Atmos. Terr. Phys. 2021. V. 221. No. 3. Art. No. 105704.
5. *Denisenko V.V., Lyakhov A.N.* // Solar-Terr. Phys. 2021. V. 7. No. 4. P. 104.
6. *Rodger C.J., Brundell J.B., Dowden R.L., Thomson N.R.* // Ann. Geophys. 2004. V. 22. P. 747.
7. *Denisenko V.V., Biernat H.K., Mezentsev A.V., Shaidurov V.A., Zamay S.S.* // Ann. Geophys. 2008. V. 26. P. 2111.
8. *Denisenko V.V.* 2-D model of the global ionospheric conductor connected with the magnetospheric conductors. Cornell University Library. 2018. http://arxiv.org/abs/1802.07955.
9. *Denisenko V.V.* // Siberian Math. J. 1994. V. 35. No. 3. P. 495.
10. *Mareev E.A.* // Phys. Uspekhi. 2010. V. 53. No. 5. P. 504.
11. *Harrison R.G.* // Surv. Geophys. 2013. V. 34. P. 209.
12. *Richmond A.D.* // J. Atmos. Terr. Phys. 1973. V. 3. No. 6. P. 1083.

Denisenko V.V, Rycroft M.J., Harrison R.G. Mathematical model of the global ionospheric electric field generated by thunderstorms *Bulletin of the Russian Academy of Sciences: Physics*. 2023. V. 87(1). 118-123.
DOI:10.3103/S1062873822700277